

Received July 21, 2021, accepted August 9, 2021, date of publication August 12, 2021, date of current version August 19, 2021.

Digital Object Identifier 10.1109/ACCESS.2021.3104338

# Design of High-Performance Scattering Metasurfaces Through Optimization-Based Explicit RCS Reduction

SLAWOMIR KOZIEL<sup>1,2</sup>, (Senior Member, IEEE), MUHAMMAD ABDULLAH<sup>1</sup>,  
AND STANISLAW SZCZEPANSKI<sup>2</sup>

<sup>1</sup>Engineering Optimization and Modeling Center, Reykjavik University, 101 Reykjavik, Iceland

<sup>2</sup>Faculty of Electronics, Telecommunications and Informatics, Gdańsk University of Technology, 80-233 Gdańsk, Poland

Corresponding author: Slawomir Koziel (koziel@ru.is)

This work was supported in part by the Icelandic Centre for Research (RANNIS) under Grant 206606051, and in part by the National Science Centre of Poland under Grant 2018/31/B/ST7/02369.

**ABSTRACT** The recent advances in the development of coding metasurfaces created new opportunities in realization of radar cross section (RCS) reduction. Metasurfaces, composed of optimized geometries of meta-atoms arranged as periodic lattices, are devised to obtain desired electromagnetic (EM) scattering characteristics. Despite potential benefits, their rigorous design methodologies are still lacking, especially in the context of controlling the EM wavefront through parameter tuning of meta-atoms. One of the practical obstacles hindering efficient design of metasurfaces is implicit handling of RCS performance. To achieve essential RCS reduction, the design task is normally formulated in terms of phase reflection characteristics of the meta-atoms, whereas their reflection amplitudes—although contributing to the overall performance of the structure—is largely ignored. As a result, the conventional approaches are unable to determine truly optimum solutions. This article proposes a novel formulation of the metasurface design task with explicit handling of RCS reduction at the level of meta-atoms. Our methodology accounts for both the phase and reflection amplitudes of the unit cells. The design objective is defined to directly optimize the RCS reduction bandwidth at the specified level (e.g., 10 dB) w.r.t. the metallic surface. The benefits of the presented scheme are twofold: (i) it provides a reliable insight into the metasurface properties even though the design process is carried out at the level of meta-atoms, (ii) the obtained design requires minimum amount of tuning at the level of the entire metasurface. None of these is possible for phase-response-based approach fostered in the literature. For practical purposes, the design is conducted using a surrogate-assisted procedure involving kriging metamodels, which enables global optimization at a low computational cost. To corroborate the utility of our formulation, a high-performance metasurface incorporating crusader-cross-shaped meta-atoms has been developed. The obtained results indicate that the system characteristics predicted at the design stage are well aligned with those of the EM-simulated structure (which is not the case for the traditional design approach). The metasurface features 10-dB RCS reduction in the frequency range of 16.5 GHz to 34.6 GHz, as validated both numerically and experimentally.

**INDEX TERMS** Radar cross section (RCS), periodic structures, design task, optimization, scattering.

## I. INTRODUCTION

With the rapid advances in the field of radar detection technology, maintaining low observability of the aircraft has become a primary concern of research within the stealth

The associate editor coordinating the review of this manuscript and approving it for publication was Guido Valerio<sup>1</sup>.

technology [1], [2]. The standard radar cross section (RCS) reduction methods are based on the shape and material stealth [3], [4]. The former has a critical impact on the aerodynamic operation and structural integrity of the aircraft, whereas the latter is affected by the supplemented weight, thickness, and cost, resulting in the inability of the method to meet a variety of stealth needs. To circumvent the aforesaid

limitations, artificially engineered materials, or metamaterials, are being incorporated as alternatives to the conventional stealth methods.

Metasurfaces, two-dimensional equivalents of metamaterials, are planar patterned structures composed of periodic lattices of meta-atoms (also referred to as unit cells) [5]. Owing to their unique abilities to control the electromagnetic (EM) wavefront, the utilization of metasurfaces in the field of stealth technology has been steadily growing [6]. Traditionally, metasurfaces capitalize on two EM mechanisms to realize RCS reduction, i.e., absorbing the incident energy [7]–[9], and scattering the energy into other directions (i.e., away from the direction of incidence) [10]–[13]. The operation of the absorbing metasurfaces is based on the concept of converting the EM energy into heat and dissipating it. On the other hand, the scattering metasurfaces adjust the spatial distribution of the backscattered EM energy by adjusting the unit cell geometry, and, therefore, control the scattering properties of the structure. Therein, the aim is to scatter the incident EM wave into a single abnormal direction. At the same time, the weight, thickness and losses of the metasurfaces can be maintained below a practically acceptable level. Nevertheless, absorbing metasurfaces are susceptible to infrared detectors, which predominantly increases their detection probability. Likewise, the single-beam scattering metasurfaces only ensure RCS reduction in a monostatic configuration; however, they are not effective to reduce bistatic RCS.

Recently, the idea of scattering manipulation has been extended to implement checkerboard metasurfaces [14], [15], which offer a control over the wavefront in a more sophisticated manner. In a checkerboard-type surfaces, the two distinct meta-atom designs are employed in an alternate arrangement, where two atoms represent two phase states (0 and  $\pi$ ) to obtain RCS reduction [14]. Notwithstanding, such architectures allow for scattering a limited number of beams towards fixed propagation directions, which limits their widespread utility. Another effort in this endeavor is the introduction of coding metasurfaces [16], [17], and diffusion metasurfaces [18], [19]. The primary advantage of coding and diffusion metasurfaces over the checkerboard type surfaces is in their capability of scattering the incident EM waves into all directions, as opposed to a few fixed propagation directions. In addition to that, coding metasurfaces are also being exploited as an absorptive surface to realize essential RCS reduction [20]. In a related vein, the concept of programmable metasurfaces [21], Huygens' metasurfaces [22], and cloaking structures [23], have also been proposed to accomplish RCS reduction.

The development of scattering metasurfaces involves handling of individual meta-atom designs, and their concurrent geometry parameters adjustment. However, the lack of efficient (presumably global) techniques to optimize individual meta-atoms under relevant constraints, as well as the entire structure, limits the performance of metasurfaces, in particular, their RCS reduction bandwidth, and the level

of the reduction peak. Therein, the primary obstacle hindering efficient design of metasurfaces is implicit handling of RCS performance. To achieve essential RCS reduction, the design task is typically formulated in terms of phase reflection characteristics of the meta-atoms. More specifically, it has been argued in the literature that 10 dB RCS reduction can be maintained over a frequency band if the phase difference between the two meta-atoms remains within the  $180^\circ \pm 37^\circ$  range [14], [15]. On the other hand, their reflection amplitudes—although contributing to the overall performance of the structure—is predominantly ignored. The work [24] presents an optimization framework for metasurfaces based on surrogate models, where the optimization formulation accounts for both the amplitude and phase of the field, however, it is silent on the RCS reduction properties of metasurfaces. As a result, the conventional approaches are unable to determine truly optimum solutions, nor to account for the relationship between the meta-atom geometry and the RCS characteristics of the metasurface. In pursuit of these, a novel formulation of the metasurface design task with explicit handling of RCS reduction at the level of meta-atoms is required. At this point, it should be emphasized that highly non-linear input-output relationships between design variables and the system responses hinders utilization of conventional optimization methods. On the one hand, the advancements in high-performance computing, both in terms of hardware and software, have resulted in more widespread use of simulation-based design procedures, principally based on rigorous numerical optimization [25]. On the other hand, direct optimization of complex structures using conventional algorithms may be prohibitively expensive, especially whenever global exploration is needed. A practical solution might be a utilization of data-driven surrogates [26], involving metamodeling [27]–[29]. Recently, data-driven techniques have been applied in many areas of science and engineering [31]–[33]. Furthermore, topology optimization has been considered as generalization of parametric optimization of the meta-atoms (and, consequently, the metasurface). Therein, the entire geometry of the structure is subject to the optimization process, which brings in additional degrees of freedom. This type of tasks is often handled using inverse modeling methods (e.g., [34], [35]).

To circumvent the implicit handling of RCS characteristics in the development of scattering metasurfaces, this article proposes a novel formulation of the metasurface design task with explicit handling of RCS reduction at the level of meta-atoms. According to our approach, both phase and reflection amplitudes of the unit cells are accounted for. The design objective is defined to directly optimize the RCS reduction bandwidth at the specified level (e.g., 10 dB) with the reference to the metallic surface. Our approach offers a reliable insight into the metasurface properties even though the design process is implemented at the level of meta-atoms. Moreover, the RCS characteristics rendered through optimization of the meta-atoms is in close resemblance to that of the entire metasurface. Hence, the latter only requires slight adjustment,



which reduces the overall computational cost of the design process. To ensure globally optimum metasurface design, the design is executed using surrogate-assisted procedure involving kriging metamodels. The practical utility of our formulation is corroborated by developing a high-performance coding metasurface including crusader-cross-shaped meta-atoms. The obtained results indicate that the system characteristics predicted at the design stage are well aligned with those of the EM-simulated structure (which is not the case for the traditional design approach). The designed metasurface features 10-dB RCS reduction in the frequency range of 16.5 GHz to 34.6 GHz, as validated both numerically and experimentally.

The technical novelty and major contributions of this article can be summarized as follows: (i) proposing a novel metasurface design task formulation with explicit handling of RCS reduction at the level of meta-atoms; (ii) corroborating the efficacy of the approach, as well as demonstrating its practical utility in the context of scattering metasurface design and optimization, and (iii) designing a high-performance coding metasurface for broadband RCS reduction by applying the proposed formulation. It should be emphasized that the presented design task formulation scheme is—to the authors best knowledge—the first endeavor in the literature to explicitly handle RCS reduction at the level of meta-atoms, which is indispensable in the development of high-quality metasurface designs.

The remaining part of the paper is organized as follows. In Section II, we described the standard metasurface design task formulations, and, subsequently, introduced the proposed approach. This is followed by an exposition of the complete optimization procedure. Section III discusses the modeling and optimization results, as well as the demonstration of the practical utility of the presented formulation through the design of a high-performance coding metasurface. The benefits of the proposed and the standard methodologies are also highlighted. Section IV provides experimental validation of the considered metasurface design, and Section V concludes the paper.

## II. DESIGN PROBLEM FORMULATION AND OPTIMIZATION METHODOLOGY

This section provides a description of the standard metasurface design task formulation. Subsequently, a novel formulation is introduced. A surrogate-assisted optimization procedure involving kriging metamodels and simulation-based refinement is also outlined. The procedure is tailored to solve the metasurface optimization problem in a global sense and computationally efficient manner. Application of the proposed approach to a coding metasurface design will be presented in Section III.

### A. METASURFACE DESIGN: STANDARD FORMULATION

The design task of a scattering metasurface is typically formulated to find a pair of meta-atom designs providing the phase

difference that remains within the range of  $180^\circ \pm 37^\circ$  over possibly broad frequency range  $F$ , as suggested in [14].

The vectors of designable variables for a pair of meta-atoms will be denoted as  $\mathbf{x}_1 = [x_{1,1} \dots x_{1,n}]^T \in X_1$  and  $\mathbf{x}_2 = [x_{2,1} \dots x_{2,n}]^T \in X_2$ , with  $X_1$  and  $X_2$  being the parameter spaces of the meta-atoms. Here, for notational simplicity the dimensionalities of both spaces are assumed to be the same; generalization for different dimensionalities is straightforward. Their phase reflection responses are  $\mathbf{R}_{P1}(\mathbf{x}_1)$  and  $\mathbf{R}_{P2}(\mathbf{x}_2)$ , respectively. The objective is to find a pair of unit cell designs  $\mathbf{x}_p^* = [(\mathbf{x}_1^*)^T (\mathbf{x}_2^*)^T]^T$  maximizing the frequency range for which the phase difference  $\Delta \mathbf{R}_P(\mathbf{x}_p) = \mathbf{R}_{P1}(\mathbf{x}_1) - \mathbf{R}_{P2}(\mathbf{x}_2)$  satisfies the condition

$$180^\circ - 37^\circ \leq \Delta \mathbf{R}_P([\mathbf{x}_1^*]^T [\mathbf{x}_2^*]^T)^T \leq 180^\circ + 37^\circ \quad (1)$$

Analytically, the design task can be formulated as follows:

$$\mathbf{x}_p^* = \arg \min_{\mathbf{x}_p \in X_1 \times X_2} U(\Delta \mathbf{R}_P(\mathbf{x}_p)) \quad (2)$$

and the objective function  $U$  is defined as

$$U(\Delta \mathbf{R}_P(\mathbf{x}_p)) = -[f_U(\mathbf{x}_p) - f_L(\mathbf{x}_p)] \quad (3)$$

where  $f_U$  and  $f_L$  are the upper and lower frequencies, respectively, defining the largest continuous range of frequencies for which the condition (1) is satisfied.

It should be emphasized that the standard design task of a scattering metasurface is merely formulated in terms of the phase reflection characteristics of the meta-atoms. The reflection amplitudes of the two atoms are implicitly assumed to be identical and equal to one. In practical implementations, these neither equal to each other nor equal to unity. Because the reflection amplitudes are contributing to the overall performance of the structure, the standard formulation fails to adequately represent the metasurface properties.

In summary, the three major issues associated with coding metasurface design based on phase reflection responses are:

- The design problem is defined over an intermediate functional space (i.e., phase characteristics rather than RCS responses). Consequently, the design found by solving (1)-(3) cannot be optimum with respect to the ultimate target, which is the RCS reduction bandwidth at the specified level (e.g., 10 dB);
- Neglecting the reflection amplitudes seriously limits the reliability of the design process.
- Handling phase characteristics does not give a proper account for the RCS performance, in particular, the RCS reduction characteristic does not have a direct counterpart at the level of unit cell (meta-atom) performance.

Addressing these issues entails the development of a novel formulation of the metasurface design task with explicit handling of RCS reduction. This will be proposed in the next section below.

### B. NOVEL METASURFACE DESIGN TASK FORMULATION

As indicated in Section II. A, the implicit handling of RCS characteristics leads to serious issues concerning the reliability of the metasurface design process. To circumvent these,

this work proposes a novel design task formulation with explicit handling of RCS reduction at the level of meta-atoms. Our approach accounts for both the reflection phases and amplitudes of the unit cells.

As indicated in [20], the RCS  $\sigma_S$  of a one-bit coding metasurface at a frequency  $f$  can be approximated as

$$\sigma_S(f) = 20 \log \left| \frac{A_1(f)e^{iP_1(f)} + A_2(f)e^{iP_2(f)}}{2} \right| \quad (4)$$

where  $A_1, A_2$  and  $P_1, P_2$  are the reflection amplitude and phase responses of a pair of meta-atom designs, respectively. In the standard formulation, the reflection amplitudes of the two atoms are assumed to be unity. Note that the amplitudes and phases are functions of the respective meta-atom parameter vectors, i.e., we have  $A_1(f, \mathbf{x}_1), P_1(f, \mathbf{x}_1)$ , and  $A_2(f, \mathbf{x}_2), P_2(f, \mathbf{x}_2)$ ; consequently, we get  $\sigma_S(f, \mathbf{x}_p)$ .

In a similar way, the RCS reduction  $\sigma_R$ , of a corresponding metasurface with the reference to the equivalent metallic surface can be obtained as

$$\sigma_R(f, \mathbf{x}_p) = \sigma_S(f, \mathbf{x}_p) - \sigma_P(f, \mathbf{x}_p) \quad (5)$$

where  $\sigma_P$  is the RCS of an metallic surface. Using (4) and (5), in this work, the coding metasurface design task is defined to directly handle the RCS characteristics by solving

$$\mathbf{x}_p^* = \arg \min_{\mathbf{x}_p \in X_1 \times X_2} U(\sigma_R(f, \mathbf{x}_p)) \quad (6)$$

with the objective function  $U$  given as

$$U(\sigma_R(f, \mathbf{x}_p)) = - [f_{\sigma_U}(\mathbf{x}_p) - f_{\sigma_L}(\mathbf{x}_p)] \quad (7)$$

where  $f_{\sigma_U}$  and  $f_{\sigma_L}$  stand for the upper and lower frequencies defining the broadest continuous frequency range of frequencies for which  $U(\sigma_R(\mathbf{x}_p))$  is above a specified target threshold (e.g., 10 dB). The negative sign in (7) transforms the maximization task into the minimization problem. In our formulation of objective function, reflection response of a given meta-atoms is obtained through EM-simulation of the unit cells. Again, the proposed design task directly optimizes the RCS reduction bandwidth at the specified level (e.g.,  $\sigma_{Rmax} = 10$  dB) w.r.t. the metallic surface.

### C. SURROGATE-ASSISTED OPTIMIZATION PROCEDURE

In practice, the design task formulated in Section II. B needs to be solved in a global sense because typical meta-atom geometries offer considerable flexibility. Consequently, identification of the region containing the optimum design is a non-trivial problem, which cannot be solved using local procedures. At the same time, direct handling of (6) at the level of EM simulation models (using, e.g., nature-inspired algorithms [36]) is normally prohibitive. In particular, vast majority of global optimization methods involve population-based nature-inspired algorithms, which process sets of candidate solutions with typical numbers of objective function evaluations from many hundreds to thousands. At the same time, metaheuristic algorithms exhibit limited repeatability of

solutions (due to stochastic components presents therein), and high dependence on the control parameter setup.

Here, in order to solve (6) in a computationally feasible manner, a surrogate-assisted procedure involving kriging metamodels [26] is applied. In this work, the surrogate is understood as a fast replacement model, which is used in place of expensive EM simulations to speed up the optimization procedures. The surrogate is constructed to predict the responses (e.g., frequency characteristics) of the system under design as a function of its designable (here, geometry) parameters so that the predictions are possibly close to those obtained using simulation. At the same time, the evaluation time of the surrogate should be considerably lower than for EM analysis.

In the global optimization process, massive references to EM analysis of the meta-atoms are replaced by the utilization of fast surrogates, here, implemented by means of kriging interpolation [26]. Kriging is a popular data-driven approach combining low-order polynomial regression with stochastic modeling or the residuals between the trend function and the training data in the form of a linear combination of basis functions controlled by a set of scaling factors (hyper-parameters) [26]. Due to low-dimensionality of the parameter space (typically meta-atom geometries feature up to three or four parameters), rendering accurate surrogates within the entire parameter space of interest is computationally feasible. The acquisition of the training data is accomplished by allocating samples within  $X_1$  and  $X_2$ , both defined by the lower and upper bounds  $\mathbf{l}_i = [l_{i,1} \dots l_{i,n}]^T$  and  $\mathbf{u}_i = [u_{i,1} \dots u_{i,n}]^T$  such that  $l_{i,l} \leq x_{i,l} \leq u_{i,l}$ ,  $l = 1, \dots, n$  and  $i = 1, 2$ . The EM model is evaluated to obtain the corresponding reflection amplitude and phase responses. The metamodels representing these responses will be denoted as  $\mathbf{S}_A$  and  $\mathbf{S}_P$ , and are constructed using the data samples  $\{\mathbf{x}^{(k)}, \mathbf{R}(\mathbf{x}^{(k)})\}_{k=1, \dots, N_i}$ , where  $\mathbf{R}_i(\mathbf{x}_{i(k)})$  denotes the EM-simulated reflection response (both the amplitude and phase) of the  $k$ th meta-atom, and  $N_i$  denotes the total number of training samples, respectively. Here, the samples are distributed on a rectangular grid and the number of grid nodes along each direction is decided by a large-scale sensitivity analysis. This design of experiments strategy is suitable for low dimensional problems. The kriging model is set up using a first-order polynomial as a trend function, and a Gaussian correlation function. The large-scale sensitivity analysis is understood here as verifying the variability of the meta atom responses when varying individual geometry parameters from their lower to upper bounds (with the remaining parameters set to the center of the domain). This gives a good idea of the sensitivity of the system characteristics with respect to particular variables across the parameter space.

Having the metamodels, the first step of the optimization process is a global, grid-constrained exhaustive search. This is followed by a local refinement, which allows us to determine the parameter vector minimizing the objective function (7), thus maximizing the RCS reduction bandwidth at the specified level  $\sigma_{Rmax}$ .

The grid-confined global exploration is implemented as follows. Let  $M_{m_1 \dots m_n}$  be a rectangular grid defined as  $\mathbf{x} \in M_{m_1 \dots m_n}$  if and only if  $\mathbf{x} = [x_1 \dots x_n]^T$  conform to  $x_k = l_k + j_k[(u_k - l_k)/m_k]$ , where  $k = 1, \dots, n$ ,  $m_k$  is a grid-defining integer for the  $k$ th variable, and  $j_k \in \{0, 1, \dots, m_k\}$ . The exhaustive search solves

$$\mathbf{x}_p^{(0)} = \arg \min_{\mathbf{x}^{(1)}, \mathbf{x}^{(2)} \in M_{m_1 \dots m_n}} U(\sigma_R(f, [(\mathbf{x}^{(1)})^T (\mathbf{x}^{(2)})^T]^T)) \quad (8)$$

In the above, to maintain the simplicity of notation, the grids for both meta-atoms are assumed to be identical. The optimum design  $\mathbf{x}_p^{(0)}$  is further adjusted using the standard gradient-based algorithm [36], again at the level of the metamodels. This is to improve the resolution beyond the initial grid  $M_{m_1 \dots m_n}$ . The computational cost of the entire optimization procedure is low, considering the fact that it is executed at the level of fast surrogates. Additionally, the search process is vectorized to further expedite its operation. Although the computational cost is front-loaded with the acquisition of the training data required by metamodel construction, it is inevitable to render the aforementioned computational benefits, and to enable global search in the first place.

The design refinement is subsequently carried out by tuning the geometry parameters of the entire metasurface at the EM level of description. As mentioned before, because the proposed formulation of the design problem offers a reliable insight into the metasurface properties even though the design process is implemented at the level of meta-atoms, the amount of this final tuning is normally minor as compared to what would be necessary in the case of the standard formulation. The last part of this section briefly describes the design closure process.

Let  $\mathbf{x}_A$  denote the aggregated designable parameter vector identified after surrogate-assisted optimization procedure and  $R_{red}(\mathbf{x}_A, f)$  denote the resultant RCS reduction over frequency  $f$ . Moreover, to efficiently administer possible discontinuities in the objective function values due to localized violations of the condition  $R_{red}(\mathbf{x}_A, f) \geq \sigma_{Rmax}$  at certain frequency subbands (cf. Fig. 1), a penalty term is introduced. This way, the violations are smoothly accommodated into the objective function, which is defined as

$$U_{RCS}(\mathbf{x}_A) = -[f_H(\mathbf{x}_A) - f_L(\mathbf{x}_A)] + \beta c_r(\mathbf{x}_A)^2 \quad (9)$$

The first component in (9) is the primary objective (RCS reduction bandwidth), whereas the second component is a penalty term with the function  $c_r$  defined as  $c_r(\mathbf{x}_A) = d_r$  if  $d_r > 0$  and zero otherwise. It is introduced to handle the detrimental violations of the acceptance threshold within the target band. The contribution of the penalty term is monitored by the factor  $\beta$ . Here,  $\beta = 1$ , but it is not critical. Nevertheless, it can be used to regulate the tolerance level of  $d_r$ .

The design refinement task is formulated as

$$\mathbf{x}_A^* = \arg \min_{\mathbf{x}_A \in X_1 \times X_2} U_{RCS}(\mathbf{x}_A) \quad (10)$$

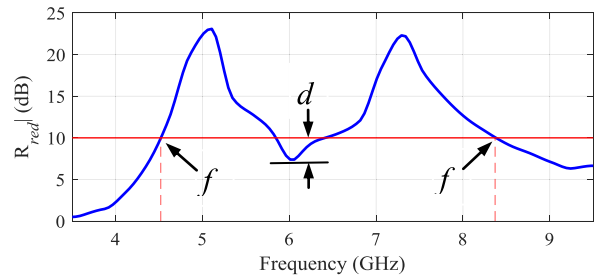


**FIGURE 1.** Exemplary RCS characteristic with  $f_L$  and  $f_U$  represent the minimum and the maximum frequency for which the condition  $R_{red}(\mathbf{x}_A, f) \geq \sigma_{Rmax}$  is satisfied, and  $d_r$  denote the maximum allowed violation within the frequency interval  $[f_L, f_U]$ .

The problem (10) is a simulation-based optimization stage (i.e., the information about the meta atom characteristics is primarily acquired from EM analysis), in which we seek for the parameter vector  $\mathbf{x}_A^*$  that maximizes the bandwidth in the sense of (9). Note that this involves independent sizing of both meta atoms (i.e., the search process is conducted over the Cartesian product of the relevant parameter spaces  $X_1$  and  $X_2$ ).

Here, the trust-region (TR) gradient-based algorithm [37] is utilized to circumnavigate the high computational cost incurred by multiple structure evaluations. Additionally, other acceleration mechanisms, i.e., the adaptive application of the rank-one Broyden formula [25] is adopted to maintain the CPU overhead to practically acceptable levels. Figure 2 shows the flow diagram of the surrogate-assisted design procedure described above.

### III. RESULTS AND DISCUSSION

This section presents the topology of the meta-atom (metasurface building block) utilized as a specific demonstration example of the design approach proposed in the work. Subsequently, the modeling and optimization results together with the performance evaluation of the optimum meta-atom designs are discussed. Finally, the practical utility and the advantages of the presented metasurface development task formulation is illustrated through the design of a complete metasurface. The detailed performance evaluation of a high-performance coding metasurface rendered by means of our approach, will be supplied in Section IV.

#### A. META-ATOM GEOMETRY

Figure 3(a) shows the meta-atom geometry considered in this work as a specific illustration example. The design shape resembles the crusader cross. The parameters  $p$ ,  $b$ , and  $d$  determine the overall structure of the meta-atom, and they are adjusted as a vector of designable variables in the optimization process. The overall size of the meta-atom is fixed to  $W \times L = 6 \times 6 \text{ mm}^2$ . As indicated in Fig. 3(b), the considered design extends ample flexibility while maintaining low dimensionality of the design space.

The latter eases the data-driven modeling procedure, in particular, ensures sufficient predictive power of the metamodels without incurring excessive computational expenses. It must

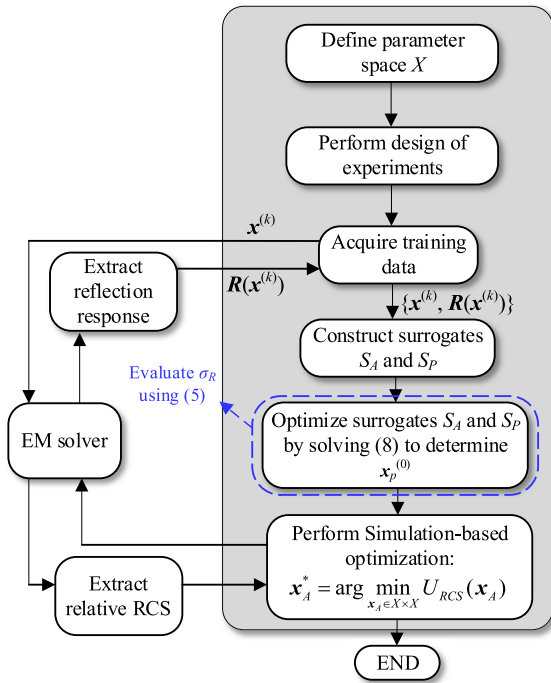


FIGURE 2. Flow diagram of a surrogate-assisted design procedure involving metamodels.

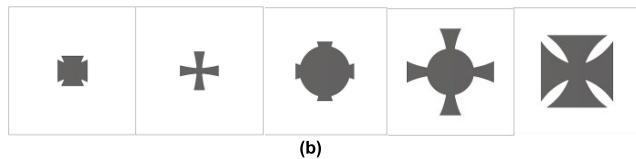
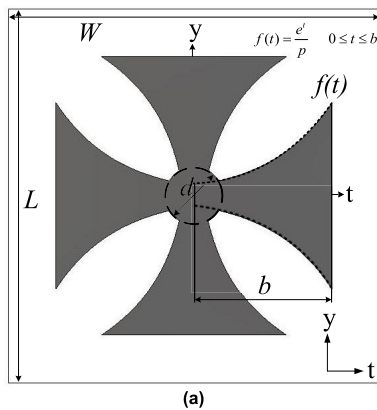


FIGURE 3. Configuration of the meta-atom considered in this work: (a) crusader cross topology, (b) five exemplary meta-atom geometries within the parameter space.

be remembered that the geometries in Fig. 3(a) and (b) visually illustrate the versatility of the considered design topology, and they do not represent the optimum designs utilized in the development of the coding metasurface. The latter will be supplied in the subsequent sub-section.

Throughout this work, a ground-backed Arlon AD250 ( $\epsilon_r = 2.5$ ,  $h = 1.5$  mm,  $\tan\delta = 0.0018$ ) is modeled as a dielectric medium. During the simulations, metallization is represented as perfect electrical conductor (PEC).

B. METAMODEL TRAINING AND VALIDATION

As mentioned in the previous section, the considered meta-atom design (cf. Fig. 1(a)) has three geometry parameters, i.e.,  $p$ ,  $b$ , and  $d$ . Therefore, the vector of designable variables is  $\mathbf{x} = [pbd]^T$ . The lower and upper limits are set to  $\mathbf{l} = [3.5 \ 0.3 \ 0.2]^T$ , and  $\mathbf{u} = [10 \ 1.6 \ 2.4]^T$ ; all dimensions are in mm. The training data is arranged on a uniform grid  $M_{7,12,7}$  (cf. Section II. C) with a total number of  $N = 588$  samples. The obtained EM-simulation data has been divided into the training (85 percent) and the testing (15 percent) data, later utilized for split-sample error evaluation. The frequency-domain solver of the CST Microwave Studio is employed to obtain the reflection (amplitude and phase) responses of the meta-atoms. It should be noted that the EM simulation model of the meta-atom contains about 22,000 mesh cells. The corresponding simulation time to compute the reflection response of a meta-atom is 70 seconds. Consequently, the overall CPU time required for training data acquisition is about eleven hours.

The absolute error of the metamodels  $S_A$  and  $S_P$  is 0.0003 0.86 degrees (averaged over the testing data) with the standard deviation of 0.0005 and 1.7 degrees, respectively. These statistics validates excellent predictive capabilities of the surrogates, especially for  $S_P$ , where the typical range of the reflection phase response exceeds 400 degrees. Further, Fig. 4 demonstrates the surrogate and the EM-simulated reflection responses for the selected test samples. As can be observed, the surrogate model responses are in excellent agreement with the corresponding EM-simulated outputs. This alignment indicates that the globally-optimum solution obtained at the level of the surrogate is likely to be located in a close vicinity of the true (i.e., EM-level) optimum.

It should be noted that, in this work, the surrogate is constructed directly for the amplitude and phase responses of the unit cell, rather than for real and imaginary parts of the electric field. The latter is typically carried out (e.g., [39]) due to the fact that real and imaginary components are smooth and of well-defined ranges. Nevertheless, here, accurate surrogates of amplitude and phase were obtained using reasonably small number of training data samples, with the reported modeling errors giving direct account of the model predictive power.

C. OPTIMIZATION RESULTS

Following the successful training and validation of the metamodels, the exhaustive search-based global optimization (cf. (8)) has been executed to obtain the optimum meta-atom designs. The optimization procedure delivers a solution as  $\mathbf{x}_1^* = [3.520.732.40]^T$  and  $\mathbf{x}_2^* = [4.22 \ 1.60 \ 2.16]^T$ . Figure 5(a) illustrates the designs topologies, labeled as Atom 0 and Atom 1.

To test the consistency of the RCS characteristics obtained by means of the proposed design problem formulation against full-wave EM simulations, the corresponding  $2 \times 2$  coding metasurface is implemented, see Fig. 5(b). The latter

MOST WIEDZY Downloaded from mostwiedzy.pl

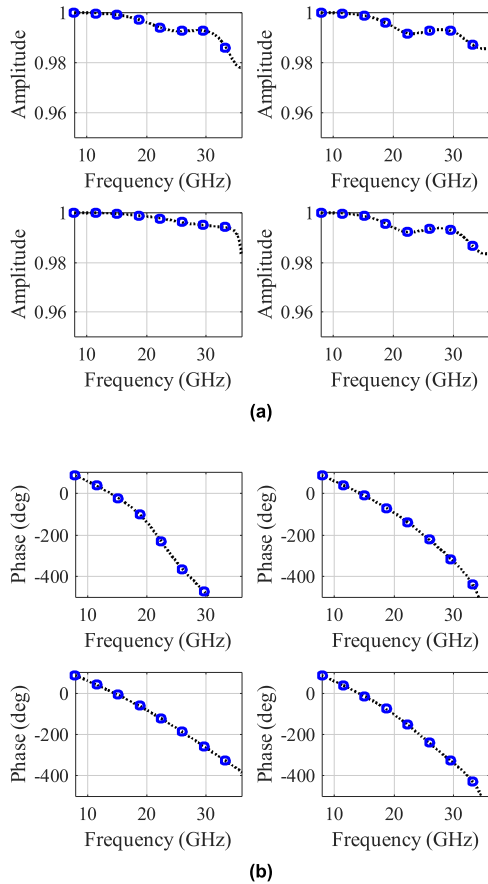


**FIGURE 4.** Performance of the surrogate models at the selected test locations; (a) amplitude ( $S_A$ ), and (b) phase reflection response predictor ( $S_P$ ). EM model (...) and surrogate responses (o).

consists of four elements: each of them contains four  $4 \times 4$  periodic lattices of Atom 0 and Atom 1. The overall size of the structure is  $W_s \times L_s = 48 \times 48 \text{ mm}^2$ . The inter-element spacing among the adjacent meta-atoms is  $s = 6 \text{ mm}$ . To evaluate the RCS reduction performance of a coding metasurface, an equivalent metallic surface is implemented to be utilized as a reference. The time-domain solver of the CST Microwave Studio is utilized for EM analysis. The EM simulation model of the metasurface presented in Fig. 5 contains about 2,400,000 mesh cells and its corresponding simulation time is 30 minutes.

Figure 6 shows the comparison between the RCS reduction performance rendered using our design problem formulation (at the level of meta-atoms), and EM-simulated RCS reduction of the metasurface. It can be observed that the two datasets decently coincide with each other. In particular, the 10-dB RCS reduction bandwidth is identical for both instances. Finally, the simulation-based local tuning is performed (cf. Section II. C) for further refinement. The obtained design is  $\mathbf{x}_A^* = [3.89 \ 1.66 \ 2.46 \ 3.87 \ 0.74 \ 2.54]^T$ . For the sake of comparison, the RCS performance before and after simulation-based refinement stage is presented in Fig. 7. As expected, the improvement at this stage is minor due to

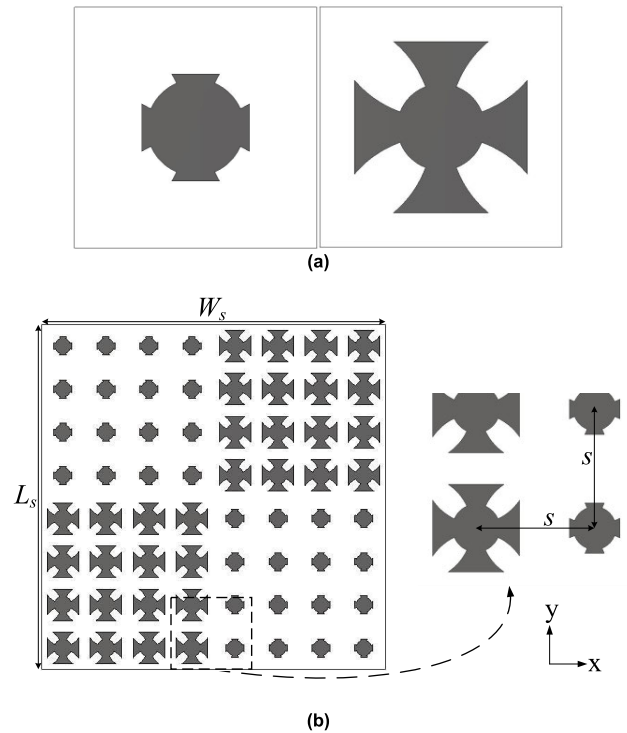


**FIGURE 5.** Optimized design solutions (upon applying surrogate-assisted optimization procedure). (a) meta-atom designs: Atom 1 (left), and Atom 0 (right), (b) configuration of a  $2 \times 2$  coding metasurface.

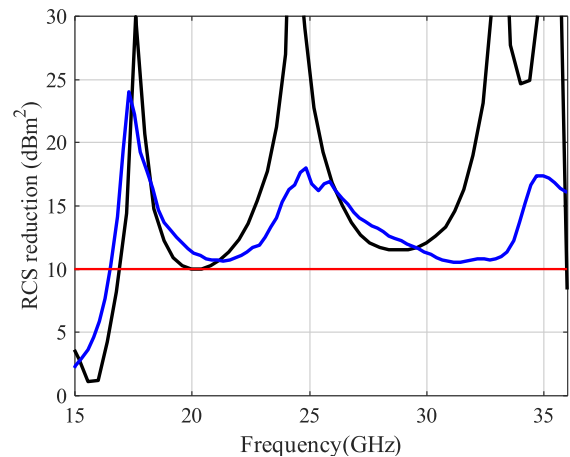


**FIGURE 6.** RCS reduction characteristic obtained at the level of meta-atoms using the proposed design problem formulation (black), and the corresponding EM-simulation response of the implemented  $2 \times 2$  metasurface (blue). The red horizontal line represents the target RCS reduction threshold, here 10-dB.

the availability of a good initial design, determined by the proposed design task formulation. It corroborates the design utility of the proposed approach. It should also be noted that certain violation of the 10 dB threshold for RCS reduction can be observed around the frequency of 35 GHz. This is due to setting the penalty coefficient  $\beta$  at relatively low value (here, 100), which makes the objective function tolerant to small violations of the threshold, while promoting bandwidth enhancement.

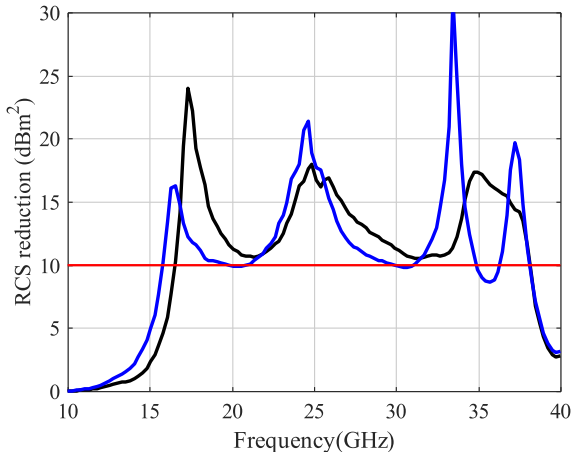


**FIGURE 7.** RCS reduction characteristic before (black), and after (blue) simulation-based local refinement. The red horizontal line represents the target RCS reduction threshold, here 10-dB.

**D. BENCHMARKING**

The metasurface design problem formulation proposed in this work has been benchmarked against the standard formulation outlined in Section II. A, where only the phase reflection response of the meta-atoms is considered. The assessment is conducted in terms of a precise account for the anticipated RCS reduction bandwidth at the level of unit cell optimization, as well as the actual RCS reduction bandwidth of the entire metasurface. Figure 8 demonstrates the reflection (amplitude and phase) performance of the optimum design solution obtained after applying global optimization procedure of Section II. C to solve the design task (2). It can be noticed that when considering the standard formulation as in (1), the anticipated 10-dB RCS reduction bandwidth extends from 16 GHz to 36 GHz. However, as presented in Fig. 9, the actual RCS reduction bandwidth of a corresponding 2 × 2 metasurface exhibits violations of the 10-dB target threshold at a significant part of the operating band, specifically from about 13 to 26 GHz, with the maximum violation of almost 3 dB. It should be reiterated that the standard formulation does not explicitly account for the RCS reduction characteristics at the level of meta-atom performance, and it only takes into account the phase reflection performance of the meta-atoms.

In other words, the performance achieved in terms of the phase responses at the level of meta-atoms does not carry over to the RCS reduction of the metasurface. On the contrary, Fig. 6 illustrates that the approximated 10-dB RCS reduction bandwidth obtained using our methodology is nearly identical to that of the actual bandwidth. Hence, it can be concluded that our methodology provides a direct account for RCS reduction performance of the metasurface, and, therefore, it is more reliable in the development of high-quality structures.

**IV. NUMERICAL AND EXPERIMENTAL VALIDATIONS**

This section presents a comprehensive description of a high-performance coding metasurface developed by applying the

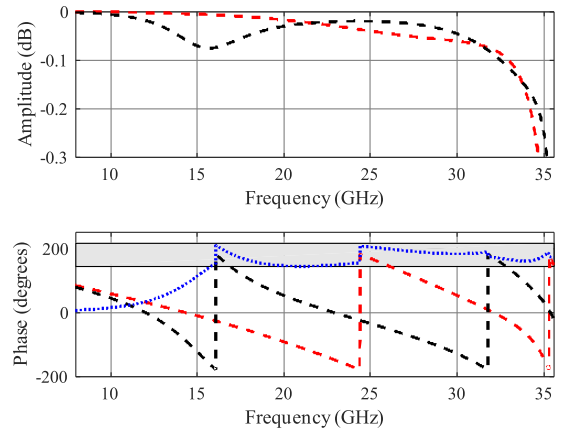


**FIGURE 8.** Reflection performance of the optimum meta-atom designs obtained using the standard formulation (cf. Section II. A): reflection amplitude (top), and reflection phase (bottom). The responses of Atom 0 and Atom 1 are marked black and red, respectively, whereas the blue curve indicates the reflection phase difference. The gray-shaded area in the bottom plot indicates the range of acceptable phase differences.

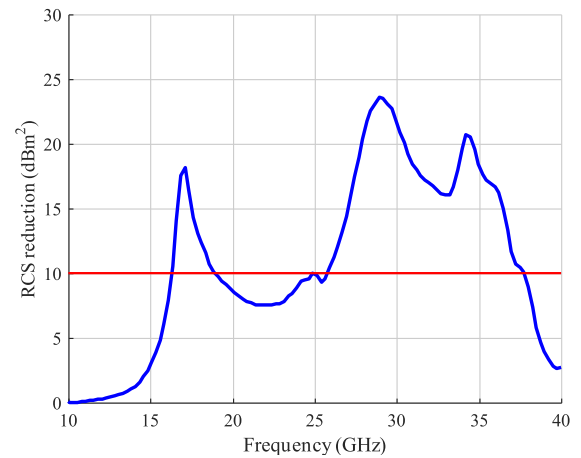


**FIGURE 9.** RCS reduction characteristics of a metasurface at the optimized meta-atom designs. The red horizontal line represents the 10-dB RCS reduction threshold relative to the PEC surface.

proposed design task formulation. The reason for conducting the optimization process at the level of a smaller, 2 × 2 metasurface, is explained, followed by a discussion on the monostatic and bistatic RCS performance of a designed 6 × 6 coding metasurface. The experimental setup is also presented, along with the measurement results of the prototyped metasurfaces.

**A. CODING METASURFACE PERFORMANCE**

So far, we considered a 2 × 2 metasurface throughout the design optimization procedure. The primary reason is that the RCS reduction performance of a metasurface is always normalized to the equivalent size metallic surface. Consequently, the size of the structure is a nominal factor. The same approach has been adopted in the literature (e.g., [14]). In particular, it has been suggested that the RCS reduction

characteristics of a  $2 \times 2$  metasurface with the reference to a metallic surface provides a decent representation of the corresponding structure of a larger size. This has been numerically corroborated through a comparative study carried out to compare the RCS reduction performance of a  $2 \times 2$  and  $6 \times 6$  metasurface, presented in Fig. 10. It can be noticed that the RCS reduction characteristics for both structures are well aligned.

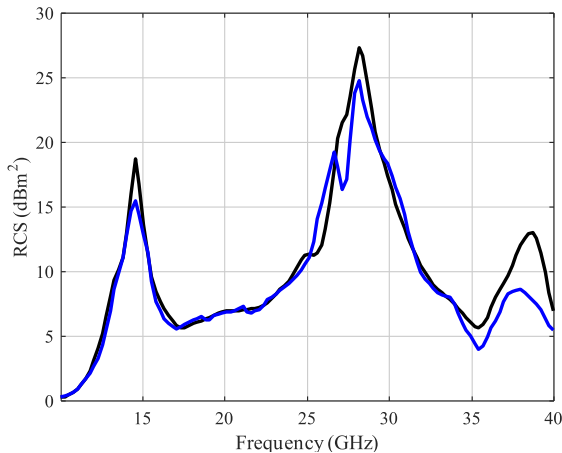


**FIGURE 10.** RCS reduction characteristics of a  $2 \times 2$  (black) and  $6 \times 6$  (blue) metasurface.

At this point, we employ the globally optimum meta-atom designs obtained in Section III to characterize a high-performance metasurface architecture featuring broadband RCS reduction. As mentioned in Section II. B, the RCS of a one-bit coding metasurface can be approximated as in (4). The underlying principle of a corresponding RCS reduction is based on the array theory [38], in particular, the entire metasurface architecture exploits the anti-phase reflection property (recall that meta-atoms are optimized to have  $180^\circ$  out-of-phase reflection) of periodic arrays to tailor the EM wavefront. Furthermore, it has been indicated in the literature that a standard checkerboard configuration disperses the incident EM energy into four pre-defined scattering lobes [15]. In a related vein, by employing lattices of ‘Atom 0’ and ‘Atom 1’ in a random configuration, more scattering lobes can be realized [16], resulting in an improved RCS reduction of the overall metasurface.

In this work, the composition of the lattices is determined by globally optimizing array factor-based approximation model (e.g., in [18]) using a binary coded genetic algorithm (GA), as presented in [18]. Figure 11 illustrates the optimized configuration of the coding metasurface comprising thirty six elements: each of them contains four  $4 \times 4$  periodic lattices of Atom 0 and Atom 1. The overall size of the structure is  $W_s \times L_s = 144 \times 144 \text{ mm}^2$ . Again, the inter-element spacing among the adjacent meta-atoms is  $s = 6 \text{ mm}$ .

To test the RCS reduction properties of a characterized metasurface, its monostatic and bistatic RCS performance

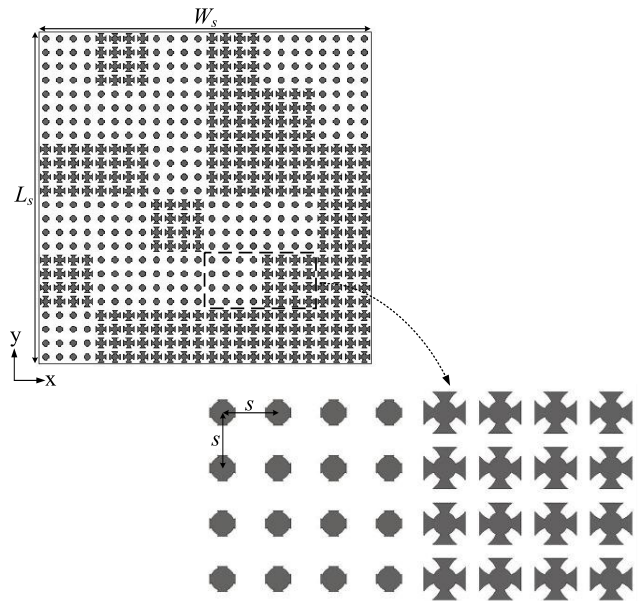


**FIGURE 11.** GA-optimized configuration of the coding metasurface.

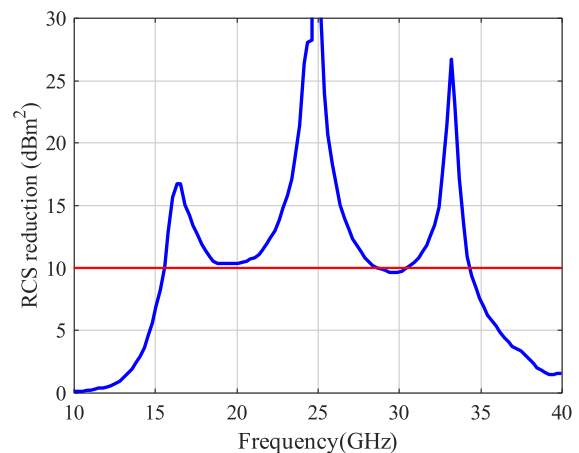


**FIGURE 12.** RCS reduction performance of the optimized configuration of a  $6 \times 6$  metasurface. The response shown is obtained through EM simulation of the structure (underlying meta-atom designs are identical to the ones given in Section III. C). The red horizontal line represents the target RCS reduction threshold.

under the plane wave incidence has been evaluated. Figure 12 shows the monostatic RCS reduction performance of a coding metasurface. It can be observed that the structure features RCS reduction in a broad frequency range, i.e., from 15.5 GHz to 34.6 GHz. Furthermore, the 3-D bistatic RCS patterns of the coding metasurface, and the equivalent size metallic surface has been illustrated in Fig. 13. It can be observed that the metallic surface causes strong reflections in the boresight direction, in a single lobe when the plane wave impinges on it. Conversely, the coding metasurface diffuses the incident wave to several directions, which results in a significant reduction of the energy in the vicinity of the scattering peak, i.e., the boresight direction.

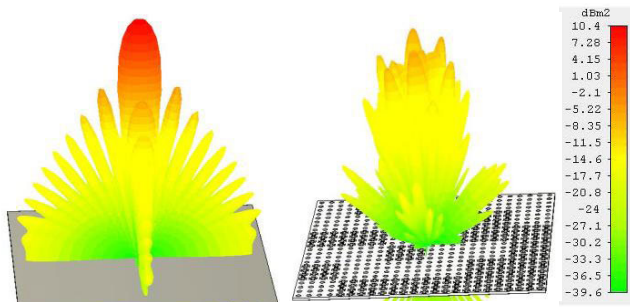


FIGURE 13. 3D scattering performance: PEC surface (left) and the coding metasurface (right). The plots correspond to the frequency of 25 GHz.

**B. EXPERIMENTAL VALIDATION**

The coding metasurface illustrated in Section. IV. A has been prototyped and measured to validate the EM simulation results. A photograph of the fabricated structure is given in Fig. 14, whereas the measurement setup is demonstrated in Fig. 15.

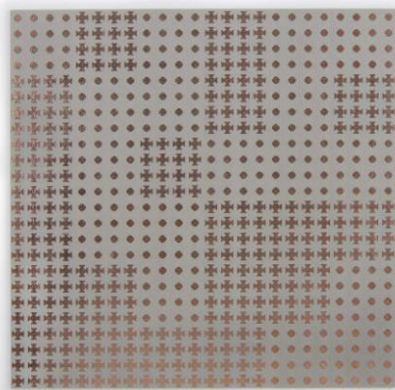


FIGURE 14. Photographs of the prototyped metasurface.

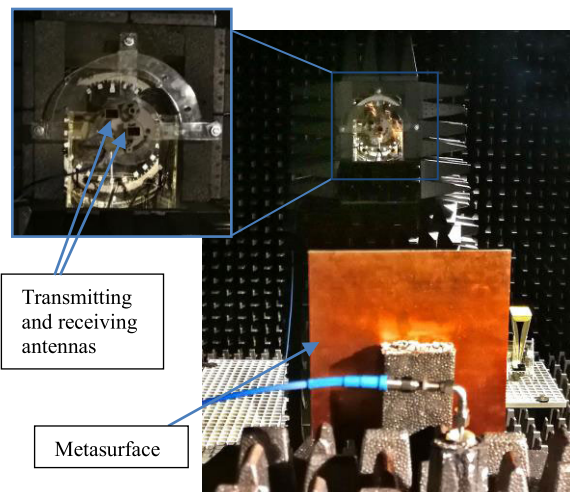


FIGURE 15. Measurement setup at Reykjavik University.

The setup includes a vector network analyzer (VNA), and a pair of linearly-polarized horn antennas (PE9850/2F-15). The two antennas are positioned perpendicular to the surface under test, among them, one of the antennas is for transmission, whereas the other one for reception of the EM waves. The experimental setup is realized in a farfield environment. The scattering performance of the metasurface under test, and the equivalent metallic surface is evaluated by measuring the transmission coefficient, captured by the VNA.

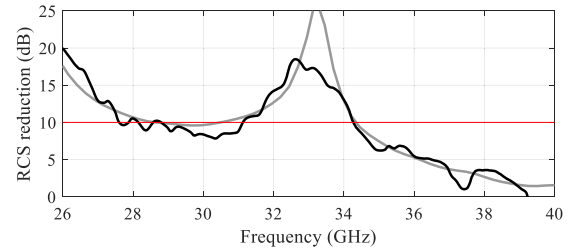


FIGURE 16. Measured (black) and simulated (gray) RCS reduction performance comparison. The red curve indicates 10-dB RCS reduction threshold.

Figure 16 shows a decent agreement between measurements and EM simulations. A slight discrepancy between the two datasets can be attributed to several reasons. Amidst, the principal factor is the spatial misalignment of the transmitting or receiving antenna with respect to surface under test. Needless to say, the precise alignment of the structure with respect to antennas (realized physically) is a challenging endeavor. A small misalignment here may lead to considerable inconsistencies. Still, the measurement results agree to 10-dB RCS reduction bandwidth obtained through EM simulation.

Due to the limited amenities available, the physical experiment is carried out in the frequency range of 26.5 GHz and 40 GHz. The above findings confirm the utility of the proposed metasurface design task formulation scheme in the context of stealth technology applications.

**V. CONCLUSION**

This article proposes a novel formulation of the metasurface design task, which enables explicit control over the RCS reduction at the level of meta-atoms. The design objective is defined to directly optimize the RCS reduction bandwidth at the specified level (e.g., 10 dB) with reference to the metallic surface. The latter is highly desirable in stealth applications. The introduced formulation account for both the reflection phases and the amplitudes of the individual meta-atoms, with the latter being typically disregarded (assumed to be equal to one) in the conventional formulation. Consequently, our approach offers a deeper insight into the entire metasurface properties even through the design process is executed at the level of unit cells.

The utility of our formulation is demonstrated by developing a high-performance coding metasurface. The final design consists of crusader-cross-shaped meta-atom designs

as a building block of the entire architecture. The design procedure is implemented using two-fold optimization, oriented toward maximization of the RCS reduction bandwidth. The initial stage employs a data-driven strategy to determine globally optimum meta-atom designs, followed by simulation-based optimization of the entire metasurface. The former involves a fast surrogate model that enables global exploration of the parameter space, otherwise unrealistic due to a massive number of EM-simulations involved. Owing to the proposed methodology, only a slight adjustment is required at the level of entire metasurface. Furthermore, the system characteristics predicted at the meta-atom design stage are well aligned with those of the EM-simulated structure, which reduces the overall computational cost of the design process. The proposed formulation has been benchmarked against standard approach demonstrated to be superior in terms of the anticipated RCS reduction bandwidth, and rendering a precise control over the RCS reduction threshold. Finally, the monostatic and bistatic performance of the coding metasurface have been briefly described. The designed metasurface features 10-dB RCS reduction in the frequency range of 16.5 GHz to 34.6 GHz. The structure has been prototyped to validate the simulation results. A good agreement between the two datasets has been observed.

It should be emphasized that the proposed methodology capitalized on a typically small number of geometry parameters describing the meta atoms. Therefore, its scalability for higher dimension will be limited. In particular, application of the approach would require a replacement of design of experiments (from grid sampling to, e.g., space-filling designs, such as Latin Hypercube Sampling, or sequential sampling methods).

## REFERENCES

- [1] E. F. Knott, *Radar Cross Section Measurements*. Springer, 2012, pp. 12–36.
- [2] P. Westwick, *Stealth: The Secret Contest to Invent Invisible Aircraft*. London, U.K.: Oxford Univ. Press, 2019, pp. 5–42.
- [3] T. A. Khan, J. X. Li, Z. Li, M. Abdullah, J. Chen, and A. X. Zhang, “Design of Vivaldi antenna with wideband reduced radar cross section,” *AEU Int. J. Electron. Commun.*, vol. 95, pp. 47–51, Oct. 2018.
- [4] H. Ahmad, A. Tariq, A. Shehzad, M. S. Faheem, M. Shafiq, I. A. Rashid, A. Afzal, A. Munir, M. T. Riaz, H. T. Haider, A. Afzal, M. B. Qadir, and Z. Khaliq, “Stealth technology: Methods and composite materials—A review,” *Polym. Compos.*, vol. 40, no. 12, pp. 4457–4472, 2019.
- [5] T. J. Cui, D. R. Smith, and R. Liu, *Metamaterials Theory, Design, and Applications*. New York, NY, USA: Springer, 2010.
- [6] A. V. Kildishev, A. Boltasseva, and V. M. Shalaev, “Planar photonics with metasurfaces,” *Science*, vol. 339, no. 6125, Mar. 2013, Art. no. 1232009.
- [7] N. I. Landy, S. Sajuyigbe, J. J. Mock, D. R. Smith, and W. J. Padilla, “Perfect metamaterial absorber,” *Phys. Rev. Lett.*, vol. 100, no. 20, pp. 207–402, 2008.
- [8] F. Costa, A. Monorchio, and G. Manara, “Analysis and design of ultra thin electromagnetic absorbers comprising resistively loaded high impedance surfaces,” *IEEE Trans. Antennas Propag.*, vol. 58, no. 5, pp. 1551–1558, May 2010.
- [9] Y. Liu and X. Zhao, “Perfect absorber metamaterial for designing low-RCS patch antenna,” *IEEE Antennas Wireless Propag. Lett.*, vol. 13, pp. 1473–1476, 2014.
- [10] X. Gao, X. Han, W.-P. Cao, H. O. Li, H. F. Ma, and T. J. Cui, “Ultrawideband and high-efficiency linear polarization converter based on double V-shaped metasurface,” *IEEE Trans. Antennas Propag.*, vol. 63, no. 8, pp. 3522–3530, Aug. 2015.
- [11] M. Paquay, J. C. Iriarte, I. Ederra, R. Gonzalo, and P. D. Maagt, “Thin AMC structure for radar cross-section reduction,” *IEEE Trans. Antennas Propag.*, vol. 55, no. 12, pp. 3630–3638, Dec. 2007.
- [12] K. Chang, “Electromagnetic gradient surface and its application to flat reflector antennas,” Ph. D. dissertation, Dept. Electr. Electron. Eng., Yonsei Univ., Seoul, South Korea, 2009.
- [13] J. C. I. Galarregui, A. T. Pereda, J. L. M. de Falcón, I. Ederra, R. Gonzalo, and P. de Maagt, “Broadband radar cross-section reduction using AMC technology,” *IEEE Trans. Antennas Propag.*, vol. 61, no. 12, pp. 6136–6143, Dec. 2013.
- [14] W. Chen, C. A. Balanis, and C. R. Birtcher, “Checkerboard EBG surfaces for wideband radar cross section reduction,” *IEEE Trans. Antennas Propag.*, vol. 63, no. 6, pp. 2636–2645, Jun. 2015.
- [15] S. H. Kim and Y. J. Yoon, “Wideband radar cross-section reduction on checkerboard metasurfaces with surface wave suppression,” *IEEE Antennas Wireless Propag. Lett.*, vol. 18, no. 5, pp. 896–900, May 2019.
- [16] L. Ali, Q. Li, T. A. Khan, J. Yi, and X. Chen, “Wideband RCS reduction using coding diffusion metasurface,” *Materials*, vol. 12, no. 17, p. 2708, Aug. 2019.
- [17] T. J. Cui, M. Q. Qi, X. Wan, J. Zhao, and Q. Cheng, “Coding metamaterials, digital metamaterials and programmable metamaterials,” *Light, Sci. Appl.*, vol. 3, no. 10, p. e218, Oct. 2014.
- [18] T. A. Khan, J. Li, J. Chen, M. U. Raza, and A. Zhang, “Design of a low scattering metasurface for stealth applications,” *Materials*, vol. 12, no. 18, p. 3031, Sep. 2019.
- [19] Y. Zhao, X. Cao, J. Gao, Y. Sun, H. Yang, X. Liu, Y. Zhou, T. Han, and W. Chen, “Broadband diffusion metasurface based on a single anisotropic element and optimized by the simulated annealing algorithm,” *Sci. Rep.*, vol. 6, no. 1, pp. 1–9, Jul. 2016.
- [20] S. Sui, H. Ma, J. Wang, Y. Pang, M. Feng, Z. Xu, and S. Qu, “Absorptive coding metasurface for further radar cross section reduction,” *J. Phys. D, Appl. Phys.*, vol. 51, no. 6, Feb. 2018, Art. no. 065603.
- [21] H. Yang, X. Cao, F. Yang, J. Gao, S. Xu, M. Li, X. Chen, Y. Zhao, Y. Zheng, and S. Li, “A programmable metasurface with dynamic polarization, scattering and focusing control,” *Sci. Rep.*, vol. 6, no. 1, pp. 1–11, Dec. 2016.
- [22] M. Chen, M. Kim, A. M. H. Wong, and G. V. Eleftheriades, “Huygens’ metasurfaces from microwaves to optics: A review,” *Nanophotonics*, vol. 7, no. 6, pp. 1207–1231, Jun. 2018.
- [23] J. Ji, J. Jiang, G. Chen, F. Liu, and Y. Ma, “Research on monostatic and bistatic RCS of cloaking based on coordinate transformation,” *Optik*, vol. 165, pp. 117–123, Jul. 2018.
- [24] R. Pestourie, C. Pérez-Arancibia, Z. Lin, W. Shin, F. Capasso, and S. G. Johnson, “Inverse design of large-area metasurfaces,” *Opt. Exp.*, vol. 26, no. 26, pp. 33732–33747, 2018.
- [25] S. Koziel and A. Pietrenko-Dabrowska, “Expedited optimization of antenna input characteristics with adaptive Broyden updates,” *Eng. Computations*, vol. 37, no. 3, pp. 851–862, Sep. 2019.
- [26] T. W. Simpson, J. D. Poplinski, P. N. Koch, and J. K. Allen, “Metamodels for computer-based engineering design: Survey and recommendations,” *Eng. with Comput.*, vol. 17, no. 2, pp. 129–150, Jul. 2001.
- [27] S. Koziel, L. Leifsson, and X. S. Yang, “Surrogate-based optimization,” in *Simulation-Driven Design Optimization and Modeling for Microwave Engineering*, S. Koziel, X. S. Yang, and Q. J. Zhang, Eds. London, U.K.: Imperial College Press, 2012, pp. 41–80.
- [28] S. Koziel and J. W. Bandler, “Reliable microwave modeling by means of variable-fidelity response features,” *IEEE Trans. Microw. Theory Techn.*, vol. 63, no. 12, pp. 4247–4254, Dec. 2015.
- [29] S. Koziel and A. Pietrenko-Dabrowska, *Performance-Driven Surrogate Modeling of High-Frequency Structures*. New York, NY, USA: Springer, 2020.
- [30] F. Feng, W. Na, W. Liu, S. Yan, L. Zhu, J. Ma, and Q.-J. Zhang, “Multifeature-assisted neuro-transfer function surrogate-based EM optimization exploiting trust-region algorithms for microwave filter design,” *IEEE Trans. Microw. Theory Techn.*, vol. 68, no. 2, pp. 531–542, Feb. 2020.
- [31] J. Peurifoy, Y. Shen, L. Jing, Y. Yang, F. Cano-Renteria, B. G. DeLacy, J. D. Joannopoulos, M. Tegmark, and M. Soljačić, “Nanophotonic particle simulation and inverse design using artificial neural networks,” *Sci. Adv.*, vol. 4, no. 6, Jun. 2018, Art. no. eaar4206.
- [32] X. Chen, W. Xue, H. Shi, L. Wang, S. Zhu, and A. Zhang, “Improving field uniformity using source stirring with orbital angular momentum modes in a reverberation chamber,” *IEEE Microw. Wireless Compon. Lett.*, vol. 29, no. 8, pp. 560–562, Aug. 2019.

- [33] X. Chen, W. Xue, H. Shi, J. Yi, and W. E. I. Sha, "Orbital angular momentum multiplexing in highly reverberant environments," *IEEE Microw. Wireless Compon. Lett.*, vol. 30, no. 1, pp. 112–115, Jan. 2020.
- [34] J. Jiang and J. A. Fan, "Simulator-based training of generative neural networks for the inverse design of metasurfaces," *Nanophotonics*, vol. 9, no. 5, pp. 1059–1069, Nov. 2019.
- [35] W. Ma, F. Cheng, Y. Xu, Q. Wen, and Y. Liu, "Probabilistic representation and inverse design of metamaterials based on a deep generative model with semi-supervised learning strategy," *Adv. Mater.*, vol. 31, no. 35, Aug. 2019, Art. no. 1901111.
- [36] A. Hoorfar, "Evolutionary programming in electromagnetic optimization: A review," *IEEE Trans. Antennas Propag.*, vol. 55, no. 3, pp. 523–537, Mar. 2007.
- [37] S. Koziel, J. W. Bandler, and Q. S. Cheng, "Robust trust-region space-mapping algorithms for microwave design optimization," *IEEE Trans. Microw. Theory Techn.*, vol. 58, no. 8, pp. 2166–2174, Jul. 2010.
- [38] A. Y. Modi, C. A. Balanis, C. R. Birtcher, and H. N. Shaman, "New class of RCS-reduction metasurfaces based on scattering cancellation using array theory," *IEEE Trans. Antennas Propag.*, vol. 67, no. 1, pp. 298–308, Jan. 2019.
- [39] S. An, C. Fowler, B. Zheng, M. Y. Shalaginov, H. Tang, H. Li, L. Zhou, J. Ding, A. M. Agarwal, C. Rivero-Baleine, K. A. Richardson, T. Gu, J. Hu, and H. Zhang, "A deep learning approach for objective-driven all-dielectric metasurface design," *ACS Photon.*, vol. 6, no. 12, pp. 3196–3207, 2019.



**SLAWOMIR KOZIEL** (Senior Member, IEEE) received the M.Sc. degree in electronic engineering from Gdańsk University of Technology, Poland, in 1995, the dual M.Sc. degree in theoretical physics and in mathematics from the University of Gdańsk, Poland, in 2000 and 2002, the Ph.D. degree in electronic engineering from Gdańsk University of Technology, in 2000, and the Ph.D. degree in mathematics from the University of Gdańsk, in 2003. He is currently a Professor with the Department of Engineering, Reykjavik University, Iceland. His research interests include CAD and modeling of microwave and antenna structures, simulation-driven design, surrogate-based optimization, space mapping, circuit theory, analog signal processing, evolutionary computation, and numerical analysis.



**MUHAMMAD ABDULLAH** received the B.Sc. degree from the University of Engineering and Technology, Pakistan, in 2016, and the M.Sc. degree from Xi'an Jiaotong University (XJTU), China, in 2019. Since late 2019, he has been associated with the Department of Engineering, Reykjavik University, Iceland, as a Researcher. From 2018 to 2019, he was with the Electromagnetics and Communication Laboratory, XJTU. On completion of M.Sc. degree, he received the Excellent Master's Thesis Award. His broader research interests include surrogate-based modeling and optimization, CAD and modeling of antennas and other high-frequency structures, simulation-driven design, machine-learning techniques, and millimeter-wave communication.



**STANISLAW SZCZEPANSKI** received the M.Sc. and Ph.D. degrees in electronic engineering from Gdańsk University of Technology, Poland, in 1975 and 1986, respectively. In 1986, he was a Visiting Research Associate with the Institute National Polytechnique de Toulouse (INPT), Toulouse, France. From 1990 to 1991, he was with the Department of Electrical Engineering, Portland State University, Portland, OR, USA, on a Kosciuszko Foundation Fellowship. From August to September 1998, he was a Visiting Professor with the Faculty of Engineering and Information Sciences, University of Hertfordshire, Hatfield, U.K. He is currently a Professor with the Department of Microelectronic Systems, Faculty of Electronics, Telecommunications and Informatics, Gdańsk University of Technology. He has published more than 160 articles and holds three patents. His teaching and research interests include circuit theory, fully integrated analog filters, high-frequency transconductance amplifiers, analog integrated circuit design, and analog signal processing.

...